XLIII CILAMCE
21–25, November, 2022
FOZ DO IGUAÇU – PR – BRAZIL

Numerical solution of single-phase flows in karstified heterogeneous carbonate rocks

Uebert G. Moreira[1], Franciane F. Rocha[1], Alfredo Jaramillo[1], Fabricio S. de Sousa[1], Roberto F. Ausas[1], Gustavo C. Buscaglia[1], Felipe Pereira[2]

[1]*Institute of Mathematical and Computer Sciences, University of São Paulo*
Av. Trabalhador São-carlense, 400, 13566-590, São Carlos, SP, Brazil
uebert.moreira@usp.br, fsimeoni@icmc.usp.br
[2]*Department of Mathematical Sciences, The University of Texas at Dallas*
800 W. Campbell Road, 75080-3021, Richardson TX, United States of America
luisfelipe.pereira@utdallas.edu

Abstract. Oil reservoirs in carbonate porous media are usually composed of several structures such as matrices, fractures and cavity systems, which impact properties like porosity, permeability and fluid transport behavior [1]. In this context, the problem of flow through a reservoir in the presence of karsts is rather challenging, and therefore the predictive capabilities related to the flow and transport processes remain severely limited. In this work, we perform simulations of a quarter of a five spot problem in a domain $\Omega \subset \mathbb{R}^2$ to numerically describe an incompressible single-phase flow in a karstified carbonate rock. The methodology is based on the geometric treatment and simulation data proposed in [2], and on the application of the Karst Index (KI) concept presented by [3]. The use of the KI follows a similar approach to the application of the Well Index presented in [4]. Given the lack of knowledge of the precise geometry of karst network shape, we test different arrangements with branching (such as in [2, 5]). The mathematical model used includes equations that describe the fluid flow through a conduit, and a mass conservation equation for each component. The domain is discretized by cartesian grids with different configurations of homogeneous and high-contrast heterogeneous media, while the governing equations are discretized by conservative finite volume methods. Results are verified in terms of conservation of mass. We compare the generated results by using Darcy's law changing the parameters of the conduit to assess its influence on the overall simulation.

Keywords: Conduit, Karst Index, carbonate rocks, Darcy flow.

1 Introduction

Reservoirs are naturally fractured, and as a consequence they have an extensive and complex system of secondary porosity [6]. Each reservoir is composed of different properties of fluid systems, fractures and cavity systems, and therefore various permeability properties and fluid transport patterns [1]. In particular, the heterogeneity arising from the presence of conduits is an essential property to be captured, because depending on the flow direction, resistance to the natural flow direction or facilitated flow channels can be identified [7]. Quantifying and predicting the behavior of hydro-mechanical parameters of these reservoirs is a major challenge for the industry.

Two main challenges are involved in the computational simulation of naturally fractured reservoirs [8]: inherent heterogeneity and uncertainties associated with the characterization of a matrix and fracture/cavity system for any field-scale problem; difficulties in conceptualizing, understanding and describing the transport flows and processes in this type of training system. As additional complexities, there is a strong coupling between the different scales of the problem and the non-linearity of the phenomena involved. In this framework, the conduit has been treated as a one-dimensional discrete hydraulics network with high permeability [9]. In addition, continuum formulations have been developed in which the mass transfer component is constitutively given in terms of an exchange coefficient, whose inverse plays the rule of a conduit resistance, multiplied by the pressure difference between the two sub-structures [10].

In practice, karst modeling is generally limited by the lack of reliable information about the geometry configuration and the computational effort required by such discretization. An alternative approach is to consider more efficient models that are placed on coarser grids, but that have the ability to reproduce with reasonable fidelity the

behavior of the original model, for example, to homogenize characteristic parameters of the geometry to reduce the geometry of a straight channel of the conduit network to one dimension. In this perspective, we seek to solve the elliptic system which defines the single-phase problem in a domain where the karst is embedded applying a model that couples 2D/1D flow system. The methodology applied here is based on the geometric treatment and simulation data proposed in [2], and on the application of the Karst Index (K_I) concept presented by [3]. The use of the K_I follows a similar approach to the application of the Well Index presented in [4]. As a way of validating the results, we verified that the masses are conserved in all elements. In addition, we observe that the behavior of the pressure, velocity and saturation fields are consistent with the expected physical behavior.

The following section will discuss the characteristics of the computational model used in this work, including geometric domain, discretization scheme, mathematical models involved in the simulation and boundary conditions. The results and discussions are discussed in section 3. Finally, in section 4, final comments and suggestions for future work are offered.

2 Mathematical setting

We begin by stating the pattern flow model and subsequently we present the formulation within the framework of homogenization to derive the coupled 2D/1D flow system given in [2]. We consider single phase incompressible flow in a carbonate matrix that contains within its domain a network of karst conduits. For the sake of simplicity, gravitational, capillary and inertial effects are neglected. The elements of the network exhibit high aspect ratio between length and hydraulic diameter, and higher permeability compared to that of the background skeleton. In order to make clear the changes present in the solution arising from the introduction of the karstic network, we consider equal permeability in all rock locations in which no karstic segment is present, thus leaving field heterogeneity represented only by the difference between the permeability of the karst and the permeability of the matrix.

Let $\Omega \subset \mathbb{R}^2$ be the microscopic domain with boundary $\partial\Omega$ which is constituted by the porous matrix and conduit system. The local hydrodynamics along with the transmission conditions are governed by the elliptic system

$$\begin{cases} \nabla \cdot \mathbf{u}_i = 0, & \text{in } \Omega, \\ \mathbf{u}_i = -\dfrac{K_i}{\mu}\nabla p_i, & i = m, k, \end{cases} \tag{1}$$

supplemented by boundary condition $\mathbf{n} \cdot \nabla p_m = 0$ on $\partial\Omega$.

In this model, $p_i, \mathbf{u}_i, K_i,\ i \in \{m, k\}$, are respectively the pore pressure, Darcy velocity and permeability in each subdomain, and μ is the fluid viscosity. We consider the application of derivation of a coupled 2D/1D reduced model posed at the intermediate (meso) scale, where the lower-dimensional conduit network is envisioned as a collection of line sources immersed in the carbonate matrix. This approach was presented in [2] in the context of this $\mathbb{R}^3 \to \mathbb{R}$-model reduction.

Thereafter we state the governing equations of the reduced mesoscopic model according to the configuration developed by [3]. Denoting γ a subdomain associated with the karst conduit network of 1D reduced objects inside Ω, the reduced equations can be obtained by averaging the flow model over the cross section area of the conduit A_k. To this end, we assume the continuity of pressure to interchange integration and differentiation in the storage component. As a final model, we seek approximate flux $\mathbf{u}_i(\mathbf{x})$ and pressure $p_i(\mathbf{x})$, $i \in \{m, k\}$, satisfying:

$$\begin{cases} \nabla \cdot \mathbf{u}_m = \dfrac{K_I}{\mu}(p_k - p_m)\delta_{km} + q\delta_m, & \text{in } \Omega, \\ \mathbf{u}_m = -\dfrac{K_m}{\mu}\nabla p_m, & \text{in } \Omega, \\ \dfrac{d\mathbf{u}_k}{ds} = -\dfrac{1}{A_k}\dfrac{K_I}{\mu}(p_k - p_m), & \text{in } \gamma, \\ \mathbf{u}_k = -\dfrac{K_k}{\mu}\dfrac{dp_k}{ds}, & \text{in } \gamma, \\ \mathbf{n} \cdot \nabla p_m = 0, & \text{on } \partial\Omega, \end{cases} \tag{2}$$

where q is a source term, K_I is the karst index and functions δ appearing described by line- or point-source Dirac

measures.

As described by [3], the computations of the karst index are carried out at the finest scale, where the local pressure and velocity profiles are computed by solving the high-fidelity diffusion equations in the matrix and computing the flow rate at the conduit interfaces. In our numerical experiments, we use the K_I's values generated by [2].

After defining the model that describes the problem, we couple the equations of local velocity and conservation of mass, resulting in a system with two equations, in addition to the boundary condition. And then, the coupled elliptic system (2) was discretized using a conservative finite volume method, in order to obtain the following linear system:

$$\begin{bmatrix} L_m & H_m \\ H_k & L_k \end{bmatrix} \begin{bmatrix} \mathbf{p}_m \\ \mathbf{p}_k \end{bmatrix} = \begin{bmatrix} \mathbf{q} \\ \mathbf{0} \end{bmatrix}. \tag{3}$$

The system (3) has order $n_k + n_m$, where n_m is the number of pressure unknowns in the porous matrix and n_k is the number of pressure unknowns in the conduit. The Lm and Lk blocks are discretizations of the Laplacian operator in 2D and 1D, respectively, while Hm and Hk are sparse blocks containing terms corresponding to the mass transfer between matrix and karst conduits. They are almost transpose of one another, differing only by the convenient treatment of bifurcations and conduit extremities.

3 Numerical experiments

In this section, we illustrate the numerical results of the coupled reduced by conducting simulations in scenarios of a box-shaped reservoir characterized by the presence of a branchwork type karst conduit in the sense of [5]. In this setting we consider the problem of a quarter of a five-spot. The values accepted as standard configuration are shown in table 1 and were extracted from [2].

Table 1. Input parameters adopted in the simulations

Domain ($L_x \times L_y$)	1 m $\times$ 1 m
Conduit radius	1e-4 m
Rock Permeability (K_m)	1e-14 m^2
Karst Permeability (K_k)	1e-9 m^2
Viscosity	1e-3 Pa s
Karst Index (K_I^1)	1.8544e-13 m^3 (for horizontal segments)
Karst Index (K_I^2)	5.9188e-13 m^3 (for diagonal segments)
Flow rate (q)	1 m^3/s

We illustrate the numerical performance of a coupled system in two scenarios that correspond to a cross section of a reservoir characterized by the presence of a branchwork-type karst conduit. The two chosen geometries inspired from [2, 5] are shown in Fig. 1. Considering the input parameters presented in Table 1, our main goal here is to analyse is to solve the elliptic system defined in the previous section in order to obtain the pressure and velocity fields. In the simulations shown in Figures (2-6) the porous matrix was discretized in 10000 uniform elements and the elements of the karst region has the size of an edge or diagonal of a cell of the matrix mesh, depending on the direction in which the karst segment crosses the matrix domain.

In the Figure 2, we present the pressure profile in the porous matrix. The numerical results behavior is consistent with the physical phenomenon: the pressure value decreases along the diagonal direction of the injector to producing well. In addition, it can be seen that when considering the existence of the conduit, the intermediate region of the domain assumes a flat shape that resembles a flat shape, indicating that the flow occurs in a more distributed way compared to the field in which there are no karstes.The perception of such differences is facilitated by the observation of the diagonal behavior of the pressure matrix going from the injection well position towards the production well, as illustrated in Fig. 3 (left). To the right in this figure is a table that shows the pressure variation between the producing well and the injection well, where it is possible to observe a relatively significant difference between the cases studied, corresponding to approximately 16% using geometry I and approximately

10% using geometry II, considering the result without conduit as a comparative reference. These results lead us to believe that the flow in a domain that contains karsts with a configuration and proportion comparable to those considered is more distributed in the directions of the branches, which can significantly impact the value of the pressure gradient.

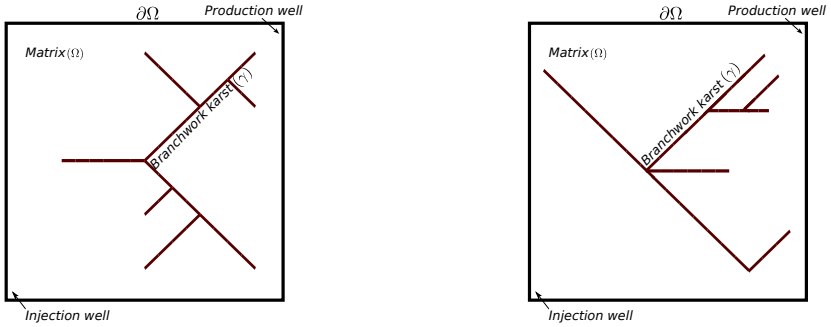

Figure 1. Sketch of the geometries considered as a representation for a branchwork-type karst conduit: Geometry I (left) and Geometry II (right) used for simulation.

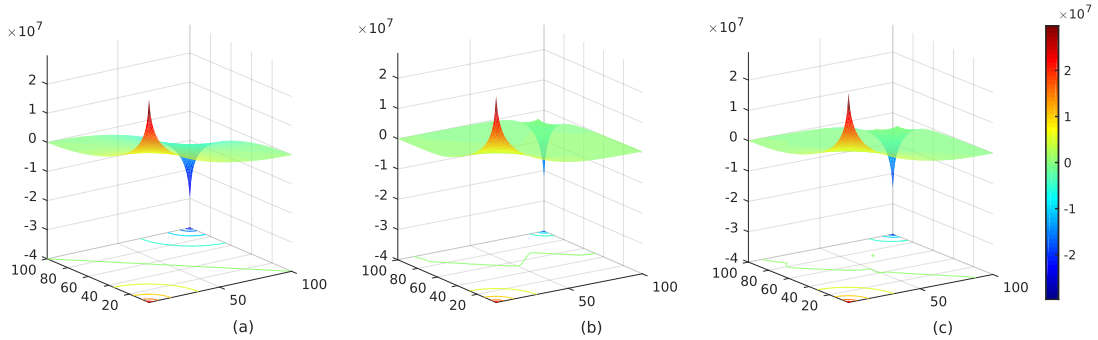

Figure 2. Pressure profile in the porous matrix for domain without conduit (left); using the Geometry I (center); using the Geometry II (right).

In turn, the velocity fields in the porous matrix region are shown in Fig. 4. In this Figure, the magnitudes of the velocity field elements are presented on a logarithmic scale. We have inserted the geometric design of the conduit geometry in violet to facilitate the physical position of the karst network in the domain. When comparing the cases studied, it is observed that each karst segment behaves as a kind of sinkhole to which the porous matrix fluid is attracted. However, following the flow trend towards the producer well, the fluid, in the intermediate regions of the karst, is transported from the karst to the matrix with a velocity lower than the velocity of entry into the karst. This is due to the amount of fluid that is transported between the internal nodes of the karst network. At the end closest to the exit of the domain fluid, the opposite occurs, the karst exit velocity is higher, probably due to the accumulation and transport of part of the fluid through the internal region of each karst segment. As a reflection of the pressure fields, the velocities in the central regions of the domain, in which there is a large presence of conduit segments, present magnitudes at levels lower than those identified by the colorimetric scale displayed in the central part of the domain in the case where there is no conduit.

With respect to the pressures inside the conduit, the Figure 5 illustrates how the values of this result are distributed considering Geometry I. The representation on the left shows the signs of the pressure values for which flow input can be interpreted at the positions of the red lines and flow output at the positions of the cyan lines. Due to the large difference in the large orders of close pressures it is interesting to use logarithmic scaling for readability purposes. Such a representation in logarithmic scale is shown on the right in this same figure. These results agree with the velocity field emphasizing the magnitudes and behavior of the flow. The pressure distribution occurs in an analogous way when considering Geometry II.

By making some modifications to the local karstic velocity equation in system (2), it is possible to study the use of a transmission factor different from the one applied in Darcy's law within the subdomain γ, such as the

factor of the Poiseuille's law. During our experiments, we performed tests to investigate the impacts of this change on velocity and pressure profiles. However, no significant difference was observed, only a proportional variation of the results presented until here. Therefore, we understand that it is not necessary to include these results here.

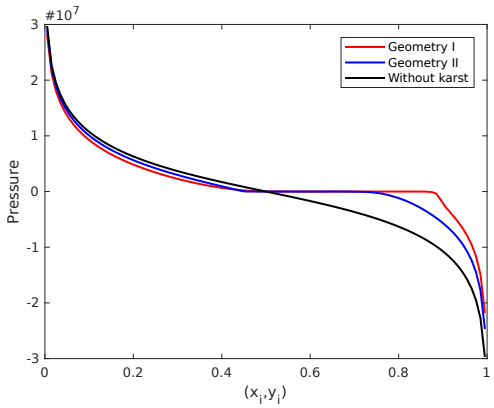

	Δp_{bh}
Without karst	5.9408e+07
Geometry I	5.0065e+07
Geometry II	5.3712e+07

Figure 3. Diagonal pressure profile in the porous matrix (left); Difference between the bottom pressures of the injection and production wells (right).

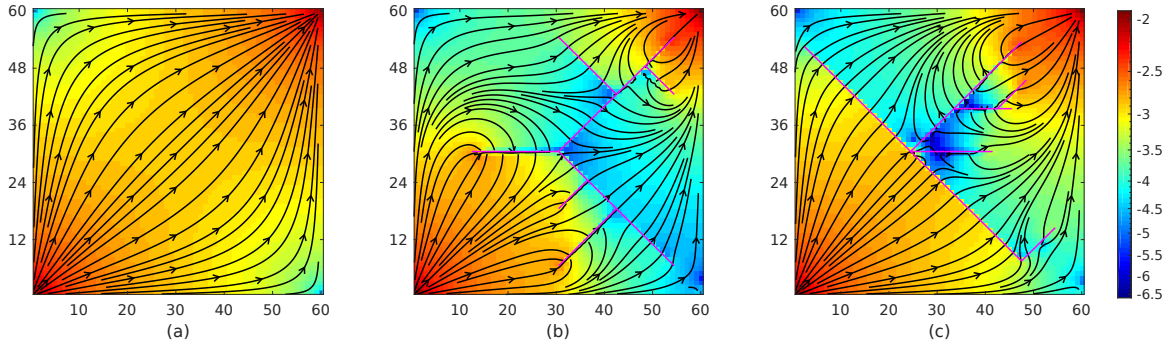

Figure 4. Log-scaled velocity fields in the porous matrix for (a) domain without conduit; (b) using the Geometry I; (c) using the Geometry II.

Finally, we tested the sensitivity of the pressure profile in relation to changes in the K_I values and K_m, keeping the other parameters as shown in Table 1. For these tests, we used the pressure behavior in the diagonal positions of the matrix that describes the pressure field as a comparative parameter. These results, presented in the Figure 6, consider simulations using geometry I since there are no changes in conclusions when observing the results generated using the other geometry. Notably, the field is more sensitive to change in porous matrix permeability than changes in K_I value.

In general, changes in the values of K_I did not affect the global amplitude of the pressure, but had an impact on images located in some segment close to the location; it was observed that as we increase the value of K_I the pressures in these regions tend to approach a constant value; on the other hand, when reducing K_I towards zero, the pressures in these regions approach the behavior observed when karst is not considered in the domain. Regarding the changes in k_m, the opposite effect was observed: There are sudden changes in the difference between the pressures at the positions of the wells, but the evolution of pressures during the domain follows a coherent variation trend.

As final experiments, we consider the 60×60 heterogeneous permeability field that indicates the permeability values in each element of the porous matrix shown in Figure 7. In this experiment, the karst is also heterogeneous so that the permeability values at each edge correspond to five orders of magnitude greater than the permeability

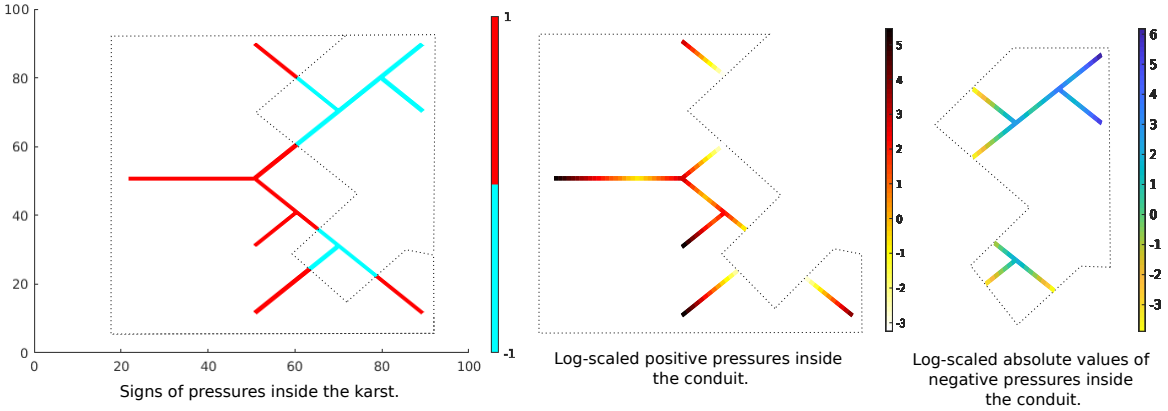

Figure 5. Pressures inside the conduit network in the shape of Geometry I.

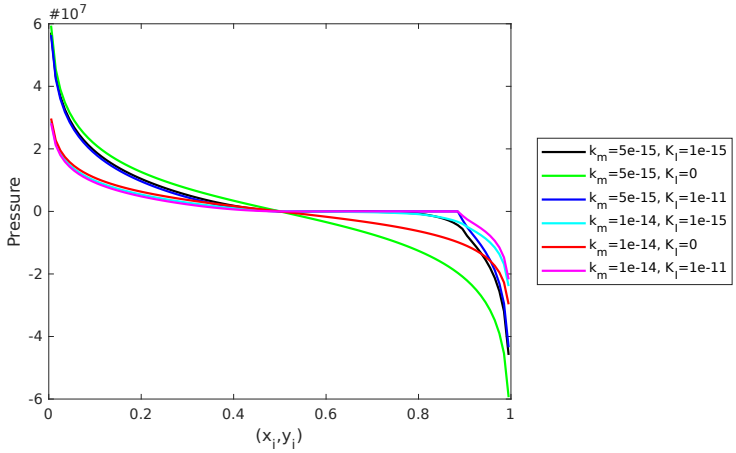

Figure 6. Diagonal pressure profile in the porous matrix with variation of parameters K_I and K_m.

value of the matrix of the cell that contains this edge. The resulting pressure and velocity fields corroborate the fields obtained when we consider homogeneous permeability fields in the subdomains if considered separately, such as illustrated in Figure 8.

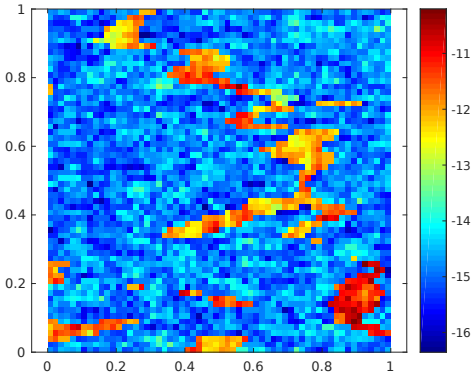

Figure 7. Log-scaled permeability field.

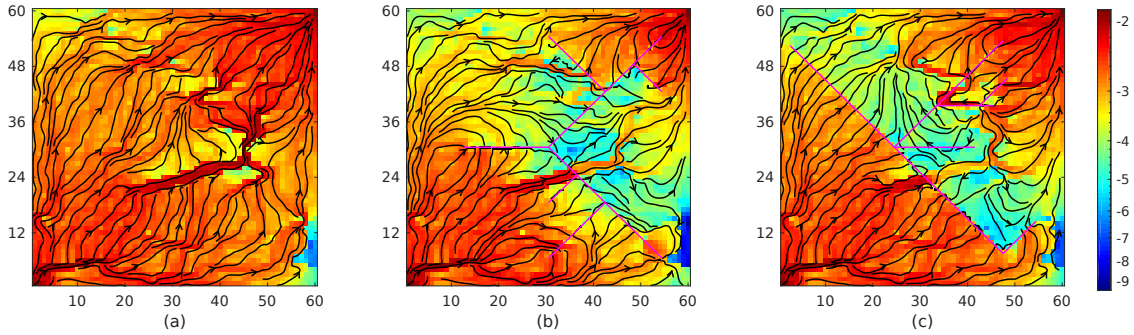

Figure 8. Log-scaled velocities of a heterogeneous field in the porous matrix for domain (a) without conduit; (b) using the Geometry I; (c) using the Geometry II.

4 Conclusions

We successfully modeled and presented results for single-phase flows in the presence of karst conduits. It is expected that the treatment presented in this work are quite promising to be applied in more robust cases of naturally fractured reservoirs. Future works include the extension to this technique for two-phase flow in a 3D domain, and has potential to be used with applications to uncertainty quantification [11], also with multiscale methods [12, 13] in parallel simulations.

Acknowledgements. We acknowledge the financial support from CAPES (Code 001).

Authorship statement. The authors hereby confirm that they are the sole liable persons responsible for the authorship of this work, and that all material that has been herein included as part of the present paper is either the property (and authorship) of the authors, or has the permission of the owners to be included here.

References

[1] C. Braester. Influence of block size on the transition curve for a drawdown test in a naturally fractured reservoir. *SPE 10543-PA*, vol. 24, n. 5, pp. 1–20, 1984.
[2] P. Ferraz, P. Pereira, E. Abreu, and M. A. Murad. Recursive mixed multiscale model reduction for karst conduit-flow in carbonate reservoirs. *Transport in Porous Media*, vol. 139, pp. 527–558, 2021.
[3] M. A. Murad, T. V. Lopes, P. A. Pereira, F. H. R. Bezerra, and A. C. Rocha. A three-scale index for flow in karst conduits in carbonate rocks. *Advances in Water Resources*, vol. 141, pp. 103613, 2020.
[4] C. Wolfsteiner, L. J. Durlofsky, and K. Aziz. Calculation of well index for nonconventional wells on arbitrary grids. *Comput. Geosci*, vol. 7, n. 1, pp. 61–82, 2003.
[5] A. N. Palmer. The origin and morphology of limestone caves. *Geol. Soc. Am. Bull*, vol. 103, pp. 1–21, 1991.
[6] D. Tiab and E. C. Donaldson. *Petrophysics. Theory and Practice of Measuring Reservoir Rock and Fluid Transport Properties*. Gulf Professional Publishing, 4 edition, 2016.
[7] S. Berrone, C. Fidelibus, S. Pieraccini, S. Scialò, and F. Vicini. Unsteady advection-diffusion simulations in complex discrete fracture networks with an optimization approach. *Journal of Hydrology*, vol. 566, pp. 332–345, 2018.
[8] Y. S. Wu. *Multiphase Fluid Flow in Porous and Fractured Reservoirs*. Gulf Professional Pub., 1 edition, 2016.
[9] Y. Cao, M. Gunzburger, F. Hua, and X. Wang. Analysis and finite element approximation of a coupled, continuum pipe-flow/darcy model for flow in porous media with embedded conduits. *Numer. Methods Partial Differ Equ.*, vol. 27, pp. 1242–1252, 2011.
[10] I. Gjerde, K. Kumar, and J. Nordbotten. A singularity removal method for coupled 1d–3d flow models. *Comput. Geosci.*, vol. 24, pp. 443–457, 2020.
[11] G. Stuart, S. Minkoff, and F. Pereira. A two-stage markov chain monte carlo method for seismic inversion and uncertainty quantification. *Geophysics*, pp. 1–66, 2019.
[12] R. T. Guiraldello, R. F. Ausas, F. S. Sousa, F. Pereira, and G. C. Buscaglia. The multiscale Robin coupled method for flows in porous media. *Journal of Computational Physics*, vol. 355, pp. 1–21, 2018.
[13] A. Francisco, V. Ginting, F. Pereira, and J. Rigelo. Design and implementation of a multiscale mixed method based on a nonoverlapping domain decomposition procedure. *Mathematics and Computers in Simulation*, vol. 99, pp. 125–138, 2014.